Strengthening of (R.C) Beams With Openings by Near Surface Mounted CFRP: Experimental study.

Ahmed Youssef Kamal , Ehab Hosny.
Lecturer : Civil Engineering Department, Higher Instituted of Technology, Benha University, EGYPT .

Abstract

This paper discusses the strengthening of (R.C) beams with openings by near surface mounted NSM system. A total number of five beams with rectangular openings in the shear zone have been tested. The opening is shown to affect the overall structural behavior of the beam. Three patterns of strengthening by NSM around the opening are investigated : horizontally, vertically and box shape. It is found that placing the NSM horizontally is not fully effective because diagonal cracks can propagate through the beam with crack path diverted to avoid intersecting with the NSM. While placing the NSM around the opening in box shape has a significant improvement in loading capacity and beam ductility. A nonlinear finite element analysis is conducted for numerical verification and extensive variable study.

Keywords: (R.C) beam, opening, strengthening, NSM

الملخص العربي

يتضمن هذا البحث دراسة علمية معملية لتأثير وجود فتحة مستطيلة في أعصاب كمرة خرسانية خلال منطقة القص على سلوك هذه الكمرة , و المحملة حتى الانهيار و طرق تقويتها باستخدام نظام NSM . أجريت هذه الدراسة على عدد خمس عينات تمثل كمرات خرسانية طولها 145 سم منها كمرة مرجعية بدون فتحات كأساس لمقارنة نتائج بقية العينات وكمرة ذات فتحة بدون تقوية لبيان مدى تأثير وجود الفتحة على السلوك الإنشائي للكمرة و ثلاث كمرات بفتحات مدعمة بأشكال مختلفة من نظام NSM (أفقية – راسية – صندوقية) .

و بناءا على نتائج هذه الدراسة تم استنتاج بعض التوصيات التي قد تساعد المهندسين عند اتخاذ أي قرار حيال وجود فتحة في أعصاب كمرة خرسانية في منطقة القص .

Introduction

Increasing requirements for existing concrete structures need enhanced strengthening methods [1] . Over the past decade, extensive research and practical application have been conducted on the strengthening of reinforced concrete structures using externally bonded fiber- reinforced polymer (FRP) laminates [2 , 3].

To improve utilization of the FRP materials, among the current methods of rehabilitation, the use of FRP bars as near surface mounted (NSM) reinforcement is now prevailing as a promising technology for increasing flexural and shear strength of deficient RC members [4,5].

Compared to externally bonded FRP reinforcement, the NSM system has a number of advantages such as NSM reinforcement is less prone to debonding from the concrete substrate, NSM bars can be more easily anchored into adjacent member to prevent debonding failures, and NSM bars are protected against environmental exposure, mechanical abrasion, fire, weather and vandalism. [2,3,6].

This technology is suitable for the repair/rehabilitation of concrete structures and has similarity to externally bonded reinforcement sheets. It is useful for improving and increasing the flexure and shear strength of structurally deficient reinforced concrete elements [7,8,9].

The method used in applying the rods is described as follows, a groove is cut in the desired direction into the concrete surface. The groove is then filled half-way with epoxy paste, the FRP rod is placed in the groove and lightly pressed. The groove is then filled with more paste and the surface is leveled [10].

Carolin and co-workers tested a series of concrete beams strengthened with near surface mounted CFRP strips. Test results demonstrated the effectiveness of the near surface mounting technique compared to the externally bonded technique [11,12].

Blaschko and Zilch carried out bond tests on carbon FRP Strips inserted inside grooves. Bond tests were conducted on double shear specimens. Test results showed that strengthening using near surface mounted CFRP strips has a greater anchoring capacity compared to externally bonded CFRP [13].

Barros and co-workers studied the strengthening technique based on near surface mounted (NSM) carbon fiber laminate strips bonded into slits opened on the concrete cover to improve the flexural capacity of columns subjected to bending and compression. The results show that a significant increase on the load carrying capacity can be achieved by using the NSM technique [14].

Tang and co-workers on their study of flexural strengthening of reinforced lightweight polystyrene aggregate concrete beams with near-surface mounted GFRP bars observed that the beams with NSM GFRP bars showed a reduction in ultimate deflection and an improvement in flexural stiffness and bending capacity, beams strengthened with NSM GFRP bars overall showed a significant increase in ultimate moment ranging from 23% to 53% over the corresponding beams without NSM GFRP bars [4].

Firas and co-workers observed that the NSM technique using CFRP rods is very effective in enhancing the flexural strength of reinforced concrete beams whatever the filling material (resin or mortar) used [15].

Barros and co-workers found that the NSM with laminates at 45° was the most effective, not only in terms of increasing beam shear resistance but also in assuring larger deformation capacity at beam failure. The NSM was also faster and easier to apply than the externally bonded FRP technique [16].
It may be sometimes necessary to make an opening in the web of the beam to allow the passage of utility ducts and pipe. Creating the opening decreases the beam ultimate load , shear capacity , change the failure mode and affect the beam ductility, strengthening by FRP rods improve the overall beam behavior [17]. So and with the above points, the specific objectives of the current study is the experimentally investigate of NSM strengthening of R.C beams with opening.

Experimental Program

The experimental program included the testing of five reinforced concrete beams, one with no opening (as reference beam), the second with opening, and three with opening strengthened by different shapes of NSM shapes (horizontal, vertical, and box). All beams have the same cross section and reinforcement arrangements, with total span of 155 cm and net span of 145 cm, the dimension of the beams cross section and reinforcement details are shown in Fig. 1. The cross section width and height is 15 and 40 cm respectively. The beams were reinforced by two bars with diameter of 10 and 12 mm as top and bottom reinforcement respectively, equivalent to the reinforcement ratio of 0.0069, while the transverse reinforcements were 6 stirrups (6-mm diameter plain round bar) spaced at 25 cm center to center. For the reference beam (B1) the loads corresponding to the yielding of main steel and shear failure were calculated according to the Egyptian code to be 11.97, 14.085 t respectively, as seen, the beam had a certain margin of safety against shear failure.
Models with opening have the same opening dimension (20 , 10 cm height and width respectively), the ratio of the opening height to the beam depth was 0.5. The opening was located at 22.5 cm from the support, at 0.31 of the shear span and at moment shear ratio of 22.5 cm , beams feature are shown in Fig. (2).
Beams B3,B4,B5 were externally strengthened around the opening with NSM system. Beam (B3) have a horizontal shape of NSM with length of 20cm (100 % of opening height) , Beam (B4) have a vertical shape of NSM with length of 30cm (150 % of opening height),while beam (B5) have a box shape of NSM. The NSM used was formed from carbon fiber-reinforced polymer rod (CFRP rod) with the following properties, nominal diameter of 0.7 cm, with fiber weight of 0.4 g/cm^2 , thickness of 0.0235 cm , tensile strength of 38736 kg/cm^2 and fiber modulus 2446500 kg/cm^2. The FRP rods were installed after the beam was cast. To install the rods , grooves were made on the surface of the beam by wood during concrete casting, then after concrete reach its compressive strength the grooves were cleaned and filled with epoxy binder compatible with the CFRP rod, then the CFRP rod (dipped in the epoxy binder) was placed into the groove.
All the beams were loaded with mid-span concentrated load ,load was measured by a load cell mounted on hydraulic jack. Deflections were measured by deflectmeters kept in positions by means of magnetic bases, two under the two opening edges

(dial 1,2) , one under the concentrated load (dial 3) and one at mid-span between the applied load and the support (dial 4), as shown in Fig. (3).
The average compressive strength of the concrete after 28 days was 310 kg/cm^2, and concrete volume weight of 2.3 kg/cm^3.
Top and bottom reinforcement bars were from high tensile steel with a modulus of elasticity of 2100000 kg/cm^2, yield stress of 3600 kg/cm^2 , while the stirrups were from mild steel with a modulus of elasticity of 2100000 kg/cm^2, yield stress of 2400 kg/cm^2.

Experimental Results and Discussion.

Failure mode and Load capacity:

The reference beam (B1) failed in flexure mode as designed with load capacity of 11t. Providing web opening (B2) change the failure mode to shear failure, due to reduction in shear capacity caused by the early formation of diagonal crack around the opening corners due to stresses concentration and the reduction in the web area. The load capacity of (B2) was 6.5t, (with drop of 41% with respect to the reference beam). Strengthening the beam with NSM system in all shapes hold the failure mode in shear failure but at a higher load compared with (B2), the shear capacity was increased in varies value due to the strengthen shape. While strengthening (horizontally, vertically and box shape) increase the load capacity to (7.25, 8 , 8.5t) respectively, with increasing percentage of (11.5 , 23 , 30.8) compared with B2, and with decreasing percentage of (34.1 , 27.3 , 22.7) compared with reference beam, Fig. (4) shows the beam failure load to the reference beam failure load percentage (P_f/P_{fr} %) . All models demonstrated no debonding failure between the concrete and the NSM.

Crack Pattern:

For (B1) the first flexure crack (C_f) occurred at 6 t at the mid-span, followed by the first diagonal crack (C_d) at 10.5 t, all cracks grew in size and number toward the load till failure, the crack pattern for (B1) shown in Fig. (5-a).
For (B2) the first flexure crack (C_f) occurred at 6 t at the mid-span, before that diagonal cracks formed at the opening upper left corner (U.L.C) at 4.5 t and extend to the applied force , in the same loading level diagonal cracks formed at the opening lower right corner (L.R.C) and extend to the support , the crack pattern for (B2) shown in Fig. (5-b). The diagonal cracks were larger and wider than the flexure cracks, and caused the stirrup near the support to be bent, which indicates shear failure , while flexure cracks delayed in grows due to the weakness in the shear capacity, as shown in Fig. (5-c).
For (B3) in which horizontal NSM was used around the opening , both flexure crack (C_f) and diagonal crack (C_d) occurred at (6 , 4.5 t) respectively, at the same load level as (B2) , which indicates that the horizontal NSM failed in delayed the formation of the diagonal cracks, the crack pattern for (B3) shown in Fig. (5-d). The increase in load capacity was due to the interruption in the diagonal crack path

caused by the NSM, but in small value because the NSM was in the same path of the crack, as shown in Fig.(5-e).
For (B4) and (B5) in which vertical and box shape of NSM respectively was used around the opening , the flexure crack (C_f) occurred at the same load level 6 t, but the crack grow and extent with increase in loading level more than (B2) , (B3) which indicate a noticeable rule of the vertical and box shape of NSM in increasing the shear capacity. The diagonal crack (C_d) was occurred at 5 t, as seen the vertical and box shape of NSM successes in delayed the initiation of the diagonal crack by 11.1% compared with (B2), the crack pattern for (B4,B5) shown in Fig. (5-f,5-h). The increase in load capacity and delayed the initiation of the diagonal crack was due to that the both strengthening system used in (B4) and (B5) intersect the natural path of the diagonal crack, which required a higher energy to redirect the path of crack propagation, in addition that in (B5) the junction of NSM increase the energy required, as shown in Fig.(5-g,5-i).

Deflection:

The load-mid-span deflection for all models are illustrated in Fig.(6), the figure illustrate the ductile (flexure) failure for (B1) and the brittle (shear) failure for the other models.
Fig.(7) shows the vertical deflection along the beam span for (B1,B2) at a certain load (4t), which indicates an excessive local deflection for (B2) at the opening zone, it has a higher deflection (about 25 % in average than that of reference beam) for (dial 1,2) due to reduction in inertia at this zone. While the increase was 16 % at the mid-span point, and decrease about 10 % at (dial 4).
Fig.(8) shows the vertical deflection along the beam span for (B2,B3,B4,B5) at a certain load (4t), which indicates that NSM existence improve (decrease) the local deflection in the opening zone and at the mid-span by about 28% in average for all shapes compared to (B2), this due to that the NSM strengthening decrease the warping of the opening.

FEM Simulation of test results:

A nonlinear finite element analysis is conducted for all experimental models by the well-known finite element structural analysis program Ansys for two purposes. The first one is to verify the simulation of the numerical model to the tested one. The second reason is to make extensive study including various factors affecting that problem that were not tested or obtained from the experiments. The second reason will be discussed in the next paper, but the first one will discuses in this part.
Solid65 is used for the three-dimensional modeling concrete material without reinforcing bars. The solid is capable of cracking (in three orthogonal directions) in tension and crushing in compression. Solid65 has eight nodes with three degrees of freedom at each node: translations in the nodal x, y, and z directions. Solid65 also was used for modeling the carbon fiber NSM. The most important aspect of this element is the treatment of nonlinear material properties.

Link8 is used for modeling the reinforcing bars. The three-dimensional spar element is a uniaxial tension-compression element with three degrees of freedom at each node: translations in the nodal x , y, and z directions, as in a pin-jointed structure, no bending of the element is considered. Plasticity, creep, and stress stiffening capabilities are included.
All materials properties were as used in experimental models, high tensile steel martial was simulated in the numerical models as Tri-linear behavior, while the mild steel and the carbon fiber material were simulated as bi-linear behavior.
The FEM results of the load capacity are compared with the experimental models in Fig.(9), a good match is obtained since the difference was not excess 8%. Also the behavior of the FEM was compared at the mid-span with the experimental models, the comparison result in a compatibility in the failure mode and deflection, as seen in Fig(10) for (B1,B2) as example, and for cracks pattern as seen in Fig(11) for (B1,B3). From previous it seem that both FEM , and experimental models have the similar responses, based on that extensive study with the FEM includes various variables will be conducts in the next paper.

Conclusions:

This paper presents an experimental study on strengthening of (R.C) beams which has a web openings with NSM system by various shapes (horizontally , vertically , box shape).
Providing an opening decreases the load capacity by 41% w.r.t that without opening, and decrease the shear capacity so that the mode of failure change from ductile flexure mode for beam without opening to brittle shear failure.
While strengthening (horizontally, vertically and box shape) with NSM system increase the load capacity by (11.5 , 23 , 30.8 %) respectively compared with beam with no strengthening system, but fail to change the mode of failure, the vertically and box shape were more effective in restore the beam load capacity by changing the diagonal cracks path than the horizontal one.
A FEM was developed and compared with the experimental models, providing good simulation for the finite element models.

References:

1- Zsombor Kálmán Szabó , György L. Balázs, “Near surface mounted FRP reinforcement for strengthening of concrete structures”, Periodica polytechnica, Civil Engineering ,51/1 , 2007,pp. 33-38.
2- De Lorenzis, L. and Teng, J.G., “Near-surface mounted FRP reinforcement: An emerging technique for strengthening structures”, Composites Part B: Engineering 38, 2007, pp. 119-143.
3- Hayder A. Rasheed , Richard R. Harrison , Robert J. Peterman , Tarek Alkhrdaji , “Ductile strengthening using externally bonded and near surface mounted composite systems”, Composite Structures 92, 2010, pp. 2379–2390.
4- Tang W.C., Balendran R.V., Nadeem A., Leung H.Y.,“Flexural strengthening of reinforced lightweight polystyrene aggregate concrete beams with near-surface mounted GFRP bars”, Building and Environment 41, 2006, pp. 1381–1393.
5- De Lorenzis L., “Strengthening of the structures with near surface mounted FRP rods”, University of Missouri-Rolla, 2000, pp. 1–153.
6- Danielle Stone, Gustavo Tumialan, Antonio Nanni, and Renato Parretti, “Near-surface mounted FRP Reinforcement : application of an emerging technology” Reinforcement &Accessories, concrete, May 2002.
7- Yan, X., B. Miller, A. Nanni, C. E. Bakis, “Characterization of CFRP rods used as near-surface mounted reinforcement ”, Proc.8th Int. Structural Faults and Repair Conf., M.C. Forde, Ed., Engineering Technics Press, Edinburgh, Scotland, 1999, 10 pp.
8- Parretti, R., Nanni, A., “Strengthening of RC Members Using Near-Surface Mounted FRP Composites: Design Overview”, Advances in structural Engineering vol.7, No.5, 2004.
9- Andrea Rizzo, Laura De Lorenzis, “Modeling of debonding failure for RC beams strengthened in shear with NSM FRP reinforcement”, Construction and Building Materials 23, 2009, pp.1568–1577.
10- De Lorenzis L., and Nanni A., “Bond Between Near Surface Mounted FRP Rods and Concrete in Structural Strengthening,” ACI Structures Journal, Vol. 99, No. 2, March-April 2002,pp. 123-133.
11- Carolin, A., Nordin, M. and Taljsten, B. , “Concrete beams strengthened with near surface mounted reinforcement of CFRP ”, Proc., Int. Conf. on FRP Composites in Civil Engineering, Research Centre for Advanced Technology in Structural Engineering, Dept. of Civil and Structural Engineering, The Hong Kong Polytechnic Univ., Hong Kong, 2001,pp. 1059–1066.
12- Hassan, T., and Rizkalla, S., “Investigation of bond in concrete structures strengthened with near surface mounted carbon fiber reinforced polymer strips”, Composites for construction journal, ASCE, August 2003, pp. 248-257.

13-Blaschko, M., and Zilch, K. , ‘‘Rehabilitation of concrete structures with strips glued into slits.’’ Proc., 12th Int. Conf. on Composite Materials, Organization of the Int. Conf. on Composite Materials, Paris,1999.
14-Barros J.A.O., Rajendra K. Varma, José M. Sena-Cruz , Alvaro F.M. Azevedo, “ Near surface mounted CFRP strips for the flexural strengthening of RC columns”, Engineering Structures 30, 2008, pp. 3412-3425.
15-Firas Al-Mahmoud , Arnaud Castel , Raoul François , Christian Tourneur, “Strengthening of RC members with near-surface mounted CFRP rods”, Composite Structures 91, 2009, pp. 138–147.
16-Barros J.A.O. , Dias S.J.E., “Near surface mounted CFRP laminates for shear strengthening of concrete beams”, Cement & Concrete Composites 28, 2006,pp. 276–292.
17- Amorn Pimanmas , “ Strengthening (R.C) beams with opening by externally installed FRP rods : Behavior and analysis”, composite structures 92 , 2010 , pp. 1957-1976.

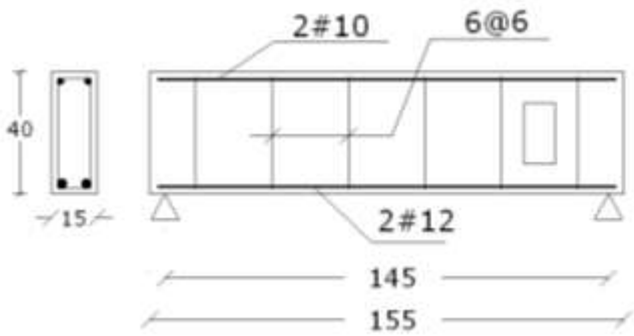

Fig.(1): Beam Dimensions and reinforcement (all Dim. In cm).

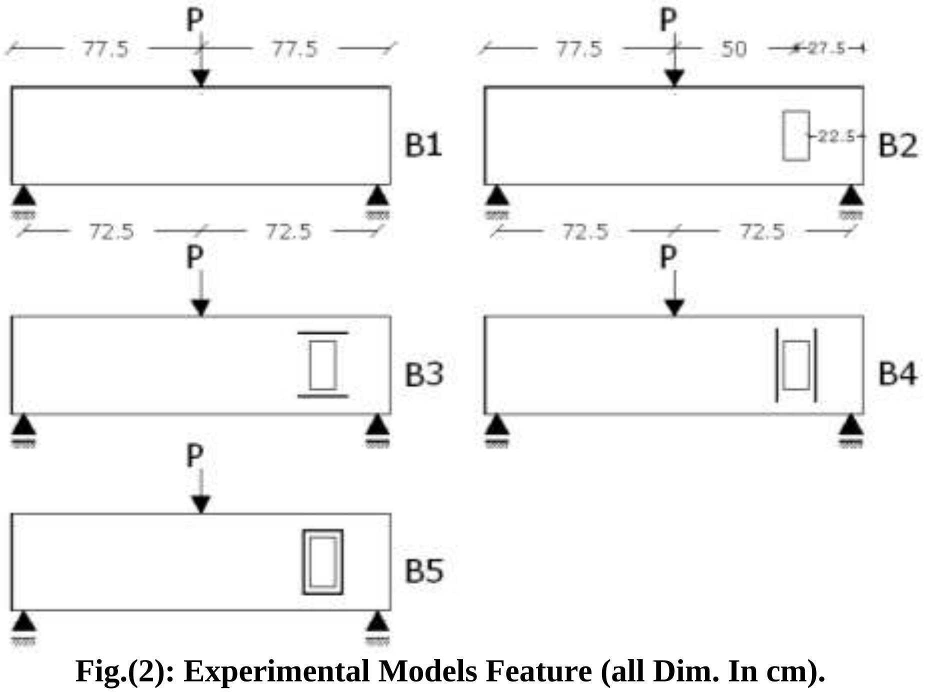

Fig.(2): Experimental Models Feature (all Dim. In cm).

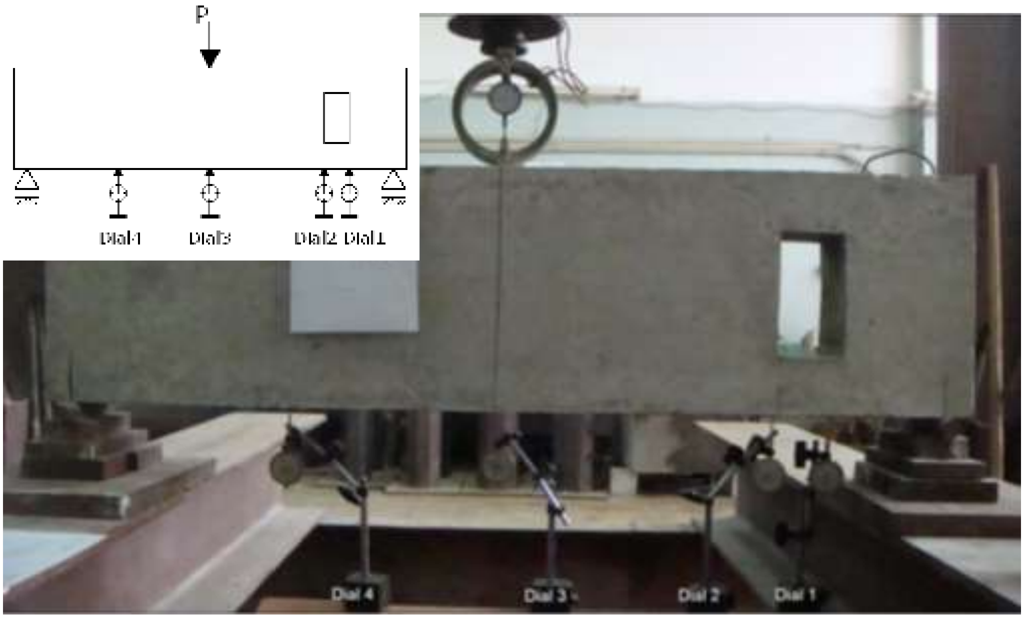

Fig.(3): Deflectmeters arrangement.

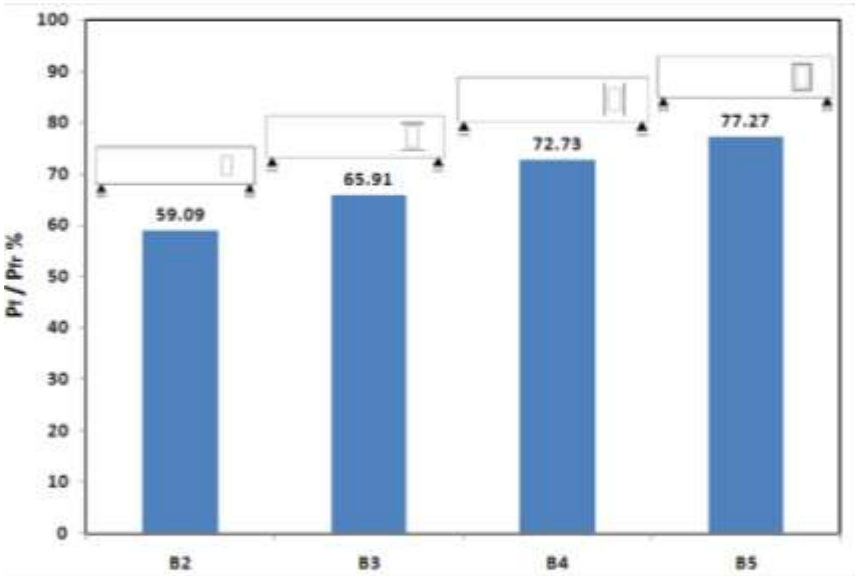

Fig.(4): Failure Loads.

Fig. (5-a).

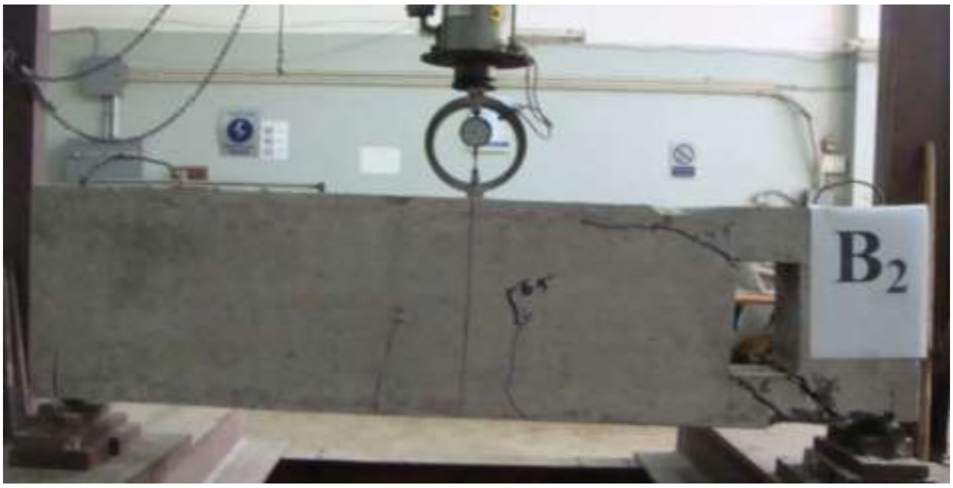

Fig. (5-b).

Fig. (5-c).

Fig. (5-d).

Fig. (5-e).

Fig. (5-f).

Fig. (5-g).

Fig. (5-h).

Fig. (5-i).

Fig.(5): Cracks Patterns of the Tested Beams.

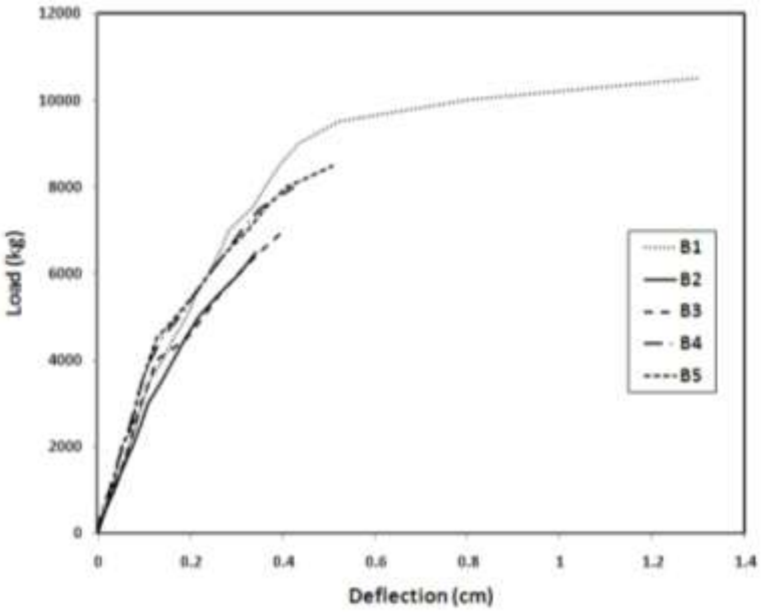

Fig.(6): Load-mid-span Deflection (dial 3).

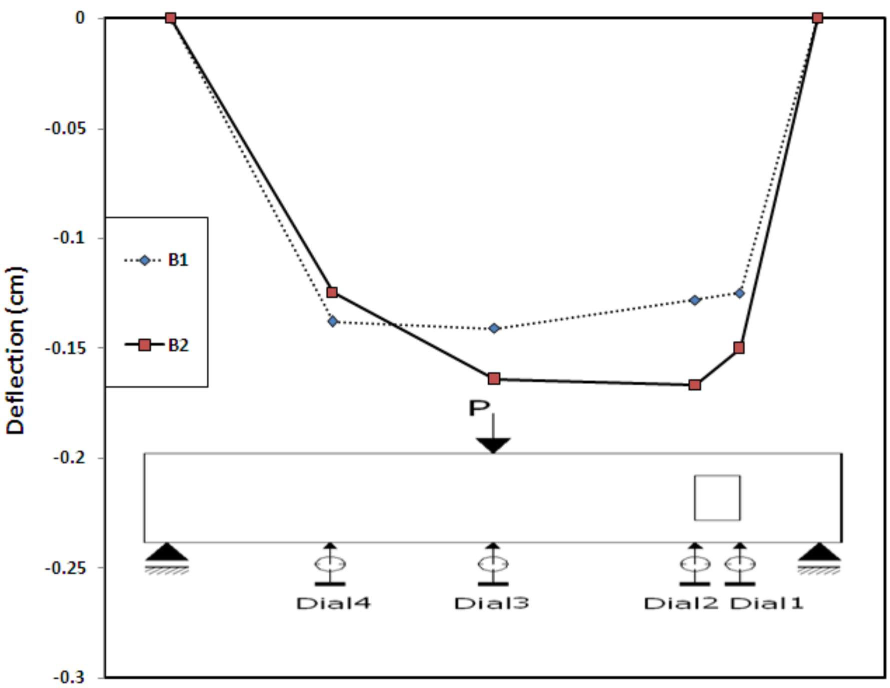

Fig.(7): Deflected Shape for (B1,B2).

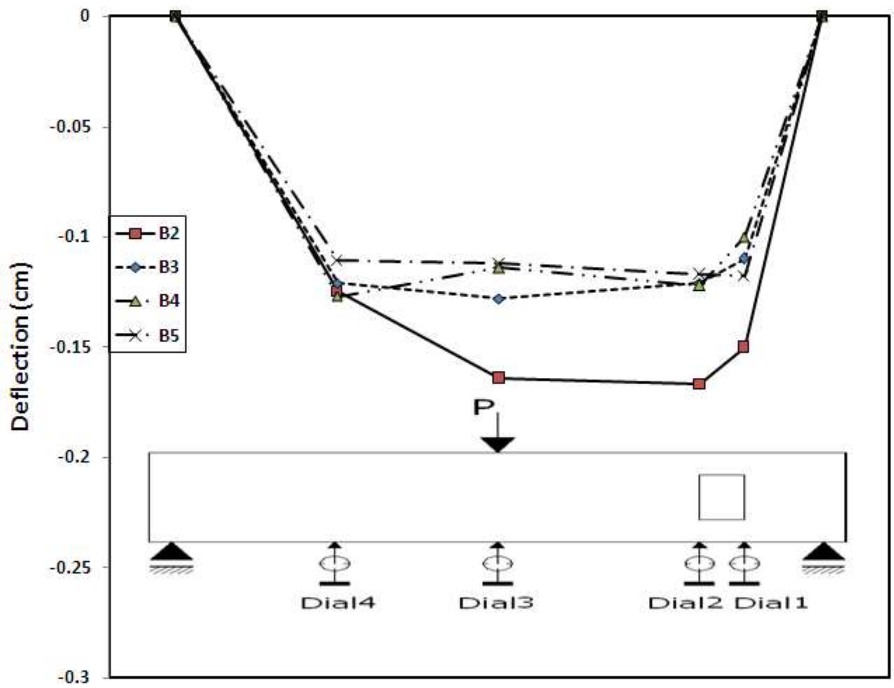

Fig.(8): Deflected Shape for (B2,B3,B4,B5).

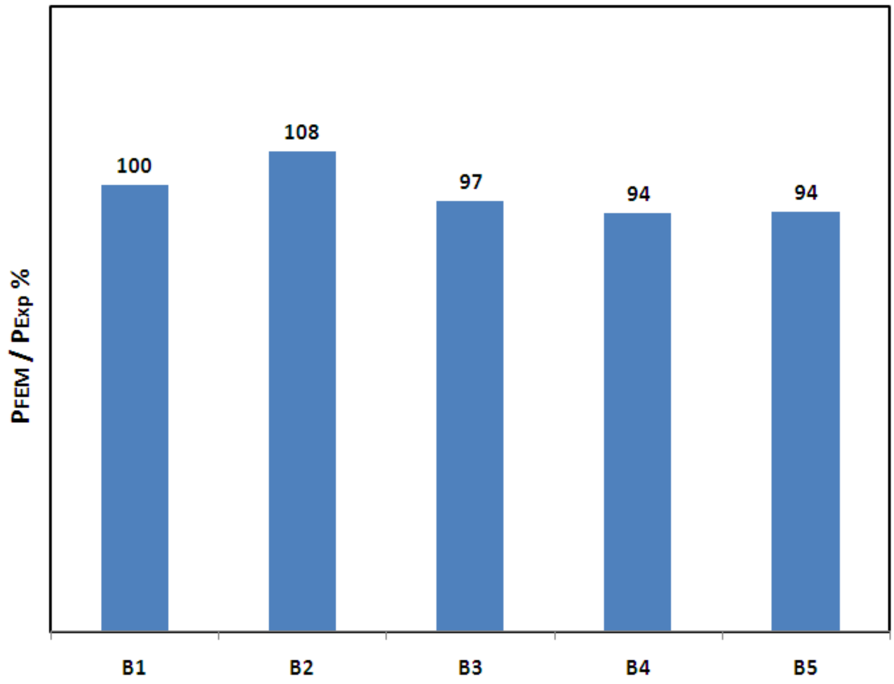

Fig.(9): Load Capacity Comparison.

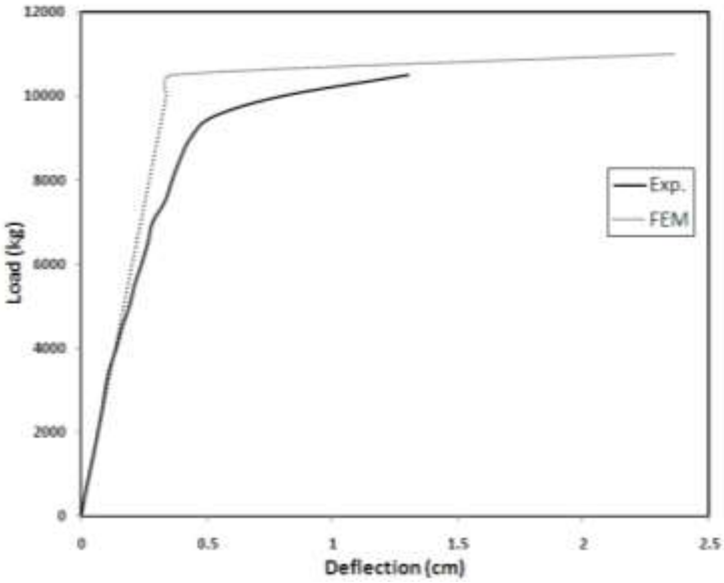

Fig.(10-a): B1

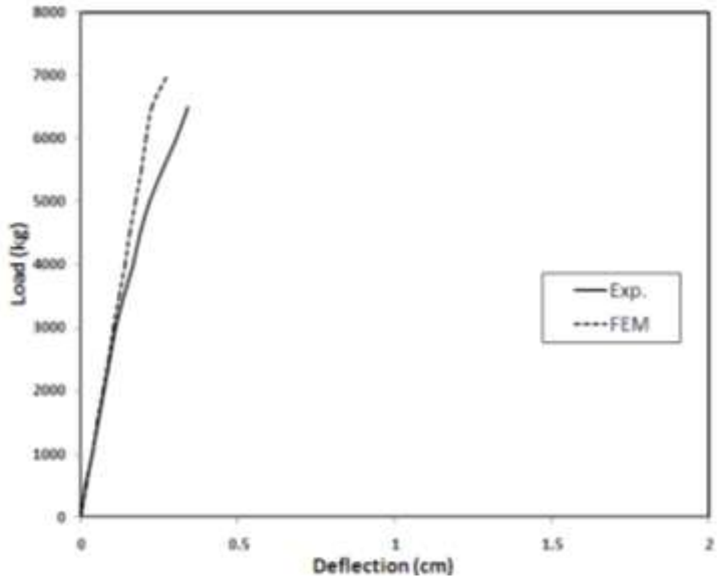

Fig.(10-a): B2

Fig.(10): Mid-span Deflection Comparison.

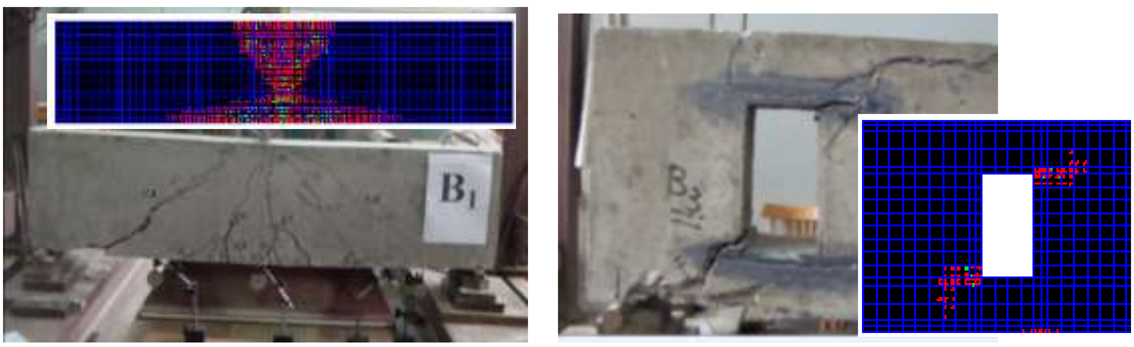

Fig.(11): Cracks Pattern Comparison (B1,B3).